OH Reaction Kinetics and Atmospheric Impact of 1-Bromopropane

David D. Nelson, Jr.,* Joda C. Wormhoudt, Mark S. Zahniser, and Charles E. Kolb

Center for Chemical and Environmental Physics, Aerodyne Research, Inc., 45 Manning Road, Billerica, Massachusetts 01821

Malcolm K. W. Ko and Debra K. Weisenstein

Atmospheric and Environmental Research, Inc., 840 Memorial Drive, Cambridge, Massachusetts 02139

Received: March 10, 1997; In Final Form: April 30, 1997[⊗]

The temperature-dependent rate constant for the reaction of the OH radical with 1-bromopropane has been measured using the discharge flow technique with laser-induced fluorescence detection of the OH radicals. Rate constants were measured as a function of temperature between $T = 271$ K and $T = 363$ K. The temperature dependence is well described by a simple Arrhenius expression, $k(T) = A \exp[-E/(RT)]$. We find that $A = (5.75 \pm 0.9) \times 10^{-12}$ cm^3 molecule^{-1} s^{-1} and $E/R = 504 \pm 50$ K for the OH reaction rate with $CH_3CH_2CH_2Br$. The reaction rate at $T = 277$ K is 9.3×10^{-13} cm^3 molecule^{-1} s^{-1}, which implies that the atmospheric lifetime for $CH_3CH_2CH_2Br$ is approximately 15 days using the scaling method of Prather and Spivakovsky. In addition, the quantitative infrared spectrum for 1-bromopropane has been obtained using a Fourier transform spectrometer. Together with the atmospheric lifetime estimate, this spectrum implies global warming potentials of 1.0, 0.3, and 0.1 for integration time horizons of 20, 100, and 500 years, respectively. We have calculated the ozone depletion potential (ODP) for bromopropane based on the kinetic results using our 2-D model and using the standard semi-empirical approach. The semiempirical calculation of the ODP, using the 15 day lifetime and the model calculated vertical profile of 1-bromopropane, gives 0.0019. However, the 2-D model result is 0.027 using a fixed mixing ratio boundary condition for 1-bromopropane. It is likely that the semiempirical method is inappropriate for species with lifetimes as short as 15 days.

Introduction

The production of chlorofluorocarbons (CFCs) and halons is being eliminated due to their adverse effects on stratospheric ozone.[1−3] In many applications previously served by CFCs and halons, partially hydrogenated halogen-containing compounds will be used as interim substitutes because of their shorter atmospheric lifetimes and consequent smaller (though still significant) impact on stratospheric ozone.[4] The reduced atmospheric lifetimes of the hydrogen-containing compounds are primarily due to their atmospheric reaction with the OH radical. Hence, measurement of the OH reaction rate coefficients for these species generally determines their atmospheric lifetimes and ozone depletion potentials (ODPs). In this paper, we examine the atmospheric impact of 1-bromopropane, a compound which will potentially be used as an industrial solvent. The emission of brominated organic compounds is particularly problematic because bromine is estimated to be ∼40−50 times more destructive to stratospheric ozone than is chlorine.[3,5] Hence, acceptable bromine compounds must have very short atmospheric lifetimes.

An additional point of concern is that halogenated compounds often strongly absorb infrared radiation and contribute to "greenhouse" radiative forcing. This property is generally quantified as the global warming potential (GWP) for the compound. The GWP depends on the atmospheric lifetime of the species as well as on its infrared spectrum. The short lifetime of 1-bromopropane leads to a favorable GWP.

In order to allow the precise calculation of the ODP and GWP for 1-bromopropane, we have measured its temperature-dependent rate constant with the OH radical, and we have quantitatively determined its infrared absorption cross sections. We present details concerning the operating conditions and the chemical purity of the sample studied in the following section.

Experimental Procedure

OH Reaction Rate Measurements. The OH reaction rate measurements were made using the discharge flow technique. In this study, the OH radicals were created in a movable source via the reaction of H atoms with NO_2. The H atoms were generated by flowing an H_2/He mixture through a 2.5 GHz microwave discharge cavity. In all cases the NO_2 concentration exceeded the H atom concentration by a factor of 2−20, and the OH formation reaction was completed within the radical source injector. The OH radicals were mixed with the reactant gas and an excess flow of carrier gas (He) in the main flow tube. This tube (diameter 2.5 cm) and the injector tube were coated with halocarbon wax to minimize OH wall losses. Flow tube temperature was regulated to within 1 K over a 50 cm reaction zone using a circulating fluid cooling/heating jacket. The temperature in the reaction zone was monitored using an alumel/chromel thermocouple.

Upon exiting the reactor flow tube, the OH radicals were detected with laser-induced fluorescence. The radicals were excited at 282 nm using the $Q_1 1$ line of the 1−0 vibrational band in the A−X electronic transition. The ultraviolet light source was a nitrogen pumped dye laser (Molectron) whose output was frequency doubled. The OH fluorescence was filtered to discriminate against scattered laser light and detected using the 1−1 and 0−0 band emission between 300 and 325 nm. The fluorescence photons were collected with appropriate imaging optics and focused onto the cathode of a Hamamatsu R212 UH photomultiplier tube. The signal from the photomultiplier was integrated with a Stanford Research Systems gated integrator and sent to a personal computer with a Lab

[⊗] Abstract published in *Advance ACS Abstracts,* June 15, 1997.

S1089-5639(97)00874-8 CCC: $14.00 © 1997 American Chemical Society

Master AD data acquisition board for signal processing. This arrangement provided a detection limit for OH radicals of ~1 × 10^8 cm^{-3} in a 1 Hz bandwidth at room temperature. This detection limit is valid for OH in a low pressure (~5 Torr or less) helium carrier gas where quenching of the OH A state is negligible.

The flow rates of the He carrier gas and of the reactants were measured using Tylan mass flow meters. These flow meters were calibrated by measuring the rate of pressure rise in a calibrated volume. Pressure measurements in the flow calibrations as well as in the kinetics experiments were made with an MKS Baratron 10 Torr capacitance manometer which was calibrated with a McLeod gauge. The helium that passed through the discharge region had a stated purity of 99.999% (Northeast Cryogenics) and was further purified by passing it through a liquid nitrogen trap with molecular sieves. The main carrier gas was helium which was delivered with a stated purity of 99.995% and used with no further purification. NO_2 (M. G. Industries, 99.5%) was also used as provided. H_2 (Air Products, 99.995%) was passed through a liquid nitrogen trap before use.

Sample purity is of considerable importance in these studies. The 1-bromopropane sample was provided by Albemarle Corp. after a careful gas chromatographic analysis. The overall purity of the sample was better than 99.9%. The three most abundant impurities were 2-bromopropane (0.04%), propanol (0.02%), and dipropyl ether (0.01%). The presence of these impurities will affect the measured rate constant by less than 0.2%. Other impurities are present at concentrations smaller than 0.01% and should also have a negligible effect on the reported rate constant.

Infrared Absorption Measurements. The infrared cross sections were measured at room temperature using a MIDAC Fourier transform infrared spectrometer. Spectra were obtained between 800 and 4000 cm^{-1} with a spectral resolution of 2 cm^{-1}. Each spectrum was the sum of 25 time domain scans; the total acquisition time for each spectrum was 25 s. The aluminum sample cell was 10 cm long with KRS5 windows sealed in place with epoxy. The cell was filled with vapor for each sample spectrum and evacuated for each background spectrum, without moving the cell. The sample pressure was measured using a 100 Torr MKS capacitance manometer. Spectra were obtained over a wide range of pressure (1−40 Torr). Fits of absorbance versus pressure were quite linear with negligible intercepts at zero pressure. The spectrometer and beam path were purged with dry nitrogen to minimize interference from atmospheric water vapor and carbon dioxide. As a further validation check of the spectrometer, the quantitative spectrum of CFC-11 was also measured under similar experimental conditions. The agreement with the accepted literature spectrum[6] was excellent.

Results

OH Reaction Rates. The experimental conditions and measured rates are presented in detail in Table 1. Fairly low hydroxyl radical concentrations ($[OH]_0 = (1-5) \times 10^{10}$ cm^{-3}) were employed. For most experiments the ratio of reactant concentration to initial OH concentration was between 10^3 and 10^4. This ratio was varied considerably with no noticeable effect on the measured rate constants, suggesting that secondary chemistry was not a source of significant error in these experiments. In addition, the pressure was varied by approximately a factor of 2 with no observed effect. The first order wall loss in these experiments varied between approximately 2 and 20 s^{-1}, with typical room temperature values of ~10 s^{-1}. The uncertainties in the rate constants in Table 1 reflect only the random errors (95% confidence limit) observed in the fits to the data.

TABLE 1: OH Reaction Rate Measurements[a]

T (K)	$k^{II} \times 10^{13}$ (cm^3 $molecule^{-1}$ s^{-1})	N	$[OH]_0 \times 10^{-10}$ (cm^{-3})	$[R] \times 10^{-13}$ (cm^{-3})	P (Torr)	V (cm/s)
271	9.1 ± 0.5	6	1	4−15	1.1	1420
273	8.8 ± 0.5	6	2	5−17	1.2	1440
294	10.5 ± 0.3	6	4	4−18	1.2, 2.3	1100, 1570
294	10.3 ± 0.5	6	5	3−14	1.1	1900
295	10.1 ± 1.0	3	2	11−16	1.15	1410
319	11.9 ± 0.5	6	4	4−15	1.1	1890
342	13.0 ± 0.3	6	4	3−14	1.1	2020
363	14.9 ± 0.8	6	2	2−12	1.1	1910

[a] Uncertainties in k^{II} reflect random error uncertainties at the 95% confidence limit.

In each experiment, the OH fluorescence signal was measured as a function of injector position or length of reaction zone. In order to provide a stable reference signal, the fluorescence intensity was measured twice at each position. The reactant flow was alternately added either upstream (S_R) or downstream (S_{He}) of the reaction zone. An equal flow of helium was alternately added with opposite phase so that the pressure in the system was constant. This switching was accomplished using computer-controlled pulsed solenoid valves. The use of this ratio technique compensates for drifts in the experimental conditions on time scales longer than the measurement period of 10 s. In particular, it guards against the effects of laser frequency drift or variation in the efficiency of OH wall removal. In addition, the sharp return of the OH signal after switching from reactant flow to helium flow suggests that the wall loss rate did not change in the presence of the reactants.

The decay of the OH signal as a function of OH source injector position in the presence of reactant appeared to be exponential. The first-order rate constant, k^{I*}, was obtained by fitting the OH signal to the following expression:

$$\frac{S_{OH}(d)}{S_{OH}(0)} = \exp\left(\frac{-k^{I*}d}{v}\right) \qquad (1)$$

where $S_{OH}(d)$ is the ratio S_R/S_{He} at reaction distance, d, and v is the average flow velocity. The data points were fit using a nonlinear weighted least-squares fit. Each data point was the average of 100 laser shots accumulated at 10 Hz. The weights for the fit were obtained from the experimentally observed scatter in the fluorescence signal. The random error uncertainties in the k^{I*} were estimated from the deviation of the data points from the curves determined in the fits. No systematic deviations were observed. A small correction factor was applied to each first-order rate constant to account for the effects of axial and radial diffusion.[7]

The bimolecular rate constants, k^{II}, were obtained from the slopes of plots of k^I versus [R], where [R] is the bromopropane concentration. The slopes were determined in linear least-squares fits, with the weights taken as the inverse squares of the k^I uncertainties. The lines were constrained to pass through the origin since significant offsets were not observed in unconstrained fits. The random error uncertainties in the k^{II} were estimated from the deviations of the k^I from the fit and are presented in Table 1. A plot of k^I versus reactant concentration is shown in Figure 1 for data taken at $T = 294$ K and at two different pressures. The reaction rate does not vary with pressure over the range studied.

The temperature dependence of the second-order rate constant is displayed in Figure 2, where we have plotted $\ln(k^{II})$ versus $1/T$. These Arrhenius plots are linear, indicating that the temperature-dependent rate constants are well represented over

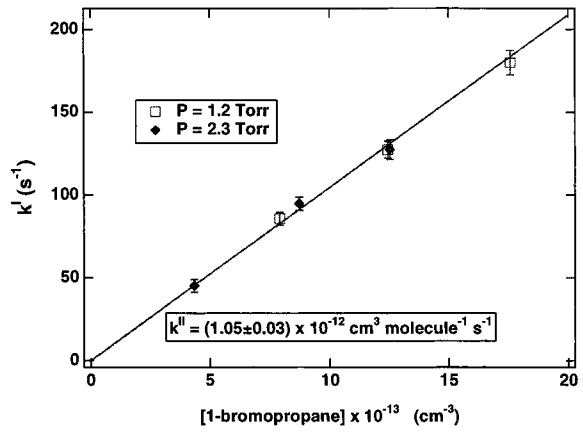

Figure 1. Plot of first-order rate constant versus 1-bromopropane concentration for reaction with OH radical at $T = 294$ K.

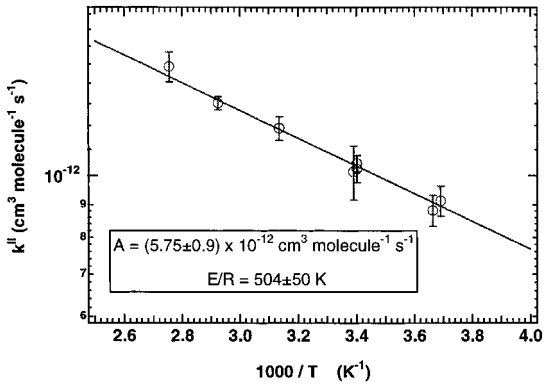

Figure 2. Arrhenius plot for the reaction of $CH_3CH_2CH_2Br$ with OH radical.

this temperature range by

$$k^{II} = A \exp(-E/RT) \qquad (2)$$

Weighted linear least-squares fits of $\ln(k^{II})$ versus $1/T$ were used to determine A and E. We report $A = (5.75 \pm 0.9) \times 10^{-12}$ cm^3 molecule^{-1} s^{-1} and $E/R = 504 \pm 50$ K for OH + $CH_3CH_2CH_2Br$. Rate constant measurements were also attempted at colder temperatures ($T = 230-250$ K), but the measurements were compromised by surface effects and the data rejected. The reported uncertainties in A and E were estimated from the deviation of the k^{II} values from the fit and reflect 95% confidence limits. We believe that systematic errors in each of the rate constant parameters A and E are small compared to the random errors. This is because A and E are correlated. The situation is the opposite with the overall rate constant because it is not correlated to another dependent variable. The random error uncertainty in the overal rate constant, k^{II}, as calculated from eq 2 is less than 3% over the temperature range studied. We estimate systematic uncertainties of ~5% for the overall rate constant and report a total uncertainty in $k^{II}(T)$ of ±6% with 95% confidence limits.

Infrared Absorption Cross Sections. The absorption cross sections derived from the measured spectra are displayed in Figure 3 as a function of frequency. Below about 860 cm^{-1} the sensitivity of the detector of our FTIR spectrometer has decreased enough that the signal-to-noise ratio of the spectrum is significantly lower, and below about 785 cm^{-1} there is no signal at all. Since 1-bromopropane has several absorption bands in this low-frequency region which will contribute to our calculation of its GWP, we extrapolated our quantitative spectrum to 500 cm^{-1} using a qualitative transmission spectrum

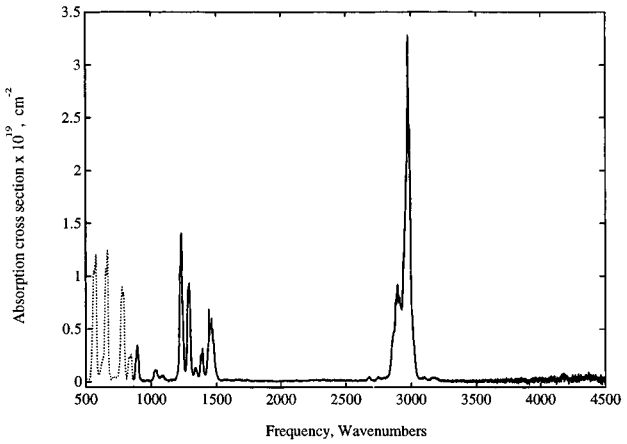

Figure 3. Quantitative infrared spectrum of 1-bromopropane. The portion of the spectrum drawn with a dotted line is an extension of our measurement which is described in the text.

printed in the Aldrich Vapor Phase FT-IR library.[8] Thus, this segment of the spectrum has some additional uncertainty. The Aldrich spectrum was used from 500 to 860 cm^{-1} and is plotted as a dotted line in Figure 3.

Discussion

Comparison with Previous Reaction Rate Measurements. We are aware of two previous studies of the OH rate constant with 1-bromopropane. Using the relative rate technique, Donaghy and co-workers[9] found a room temperature rate constant of $(1.18 \pm 0.3) \times 10^{-12}$ cm^3 molecule^{-1} s^{-1} at $T = 300$ K. This is consistent with the value calculated from the Arrhenius expression of this work, $k^{II}(T=300) = (1.07 \pm 0.06) \times 10^{-12}$ cm^3 molecule^{-1} s^{-1}. In addition, Téton et al.[10] have measured the temperature-dependent rate constant using the pulsed laser photolysis−laser-induced fluorescence technique. They find $k^{II}(T) = (5.29 \pm 0.29) \times 10^{-12} \exp[(-456 \pm 31)/T]$ cm^3 molecule^{-1} s^{-1}, which is in excellent agreement with our results.

It is also interesting to compare our rate expression with that for the reaction of OH with propane. The recommended expression is[11] $k^{II}(T) = 1.0 \times 10^{-11} \exp(-660/T)$ cm^3 molecule^{-1} s^{-1}, with $k^{II}(T=300) = 1.1 \times 10^{-12}$ cm^3 molecule^{-1} s^{-1}. The primary bromine atom substitution has only a small effect on the overall reaction rate and its temperature dependence. This is probably coincidental, since it is expected that the presence of the Br atom enhances reactivity at C_1 and suppresses reactivity at C_2.

Bromopropane Atmospheric Lifetime, GWP, and ODP Estimates. The rate constants measured in this work may be used to estimate the tropospheric lifetime of 1-bromopropane with respect to removal by reaction with OH radical. We define the tropospheric lifetime as the ratio of the total atmospheric burden of the species divided by its integrated tropospheric loss rate. Hence, the tropospheric lifetime is always greater than or equal to the atmospheric lifetime. For 1-bromopropane, the tropospheric lifetime is essentially equal to the total atmospheric lifetime. Following the approach of Prather and Spivakovsky,[12] we use the OH rate constant at 277 K to estimate lifetimes. The tropospheric lifetime, τ_x, is calculated from the OH reaction rate, k_x, via the simple procedure of scaling from the methyl chloroform tropospheric lifetime of Prinn and co-workers[13] and its OH reaction rate constant:[11]

$$\tau_x = \left[\frac{k_{mc}(T=277)}{k_x(T=277)}\right]\tau_{mc} \qquad (3)$$

where $k_{mc}(T=277)$ is the methylchloroform rate constant with OH radical at 277 K (6.7×10^{-15} cm^3 molecule^{-1} s^{-1}) and τ_{mc} is the methylchloroform tropospheric lifetime with respect to OH reaction. We estimate τ_{mc} as 5.7 years by modifying the measured atmospheric lifetime of 4.8 years to remove the contributions of stratospheric loss ($\tau \sim 50$ years)[2] and oceanic loss ($\sim$85 years)[13,14] of methylchloroform. The OH reaction rate with 1-bromopropane at 277 K is calculated from the Arrhenius expression as 9.3×10^{-13} cm^3 molecule^{-1} s^{-1}. This implies a tropospheric lifetime of only about 15 days. Thus, reaction with tropospheric OH should be, by far, the dominant atmospheric sink.

This atmospheric lifetime can be used to calculate the GWP for 1-bromopropane. The measured IR cross sections were used in the AER 1-D RC model to obtain a radiative forcing of 0.011 K/ppbv. Note that the forcing is about a factor of 10 smaller than that of CFC-11 ($CFCl_3$). Using the method outlined in ref 15, a lifetime of 15 days would imply global warming potentials of 1.0, 0.3, and 0.1 for integration time horizons of 20, 100, and 500 years, respectively.

We have calculated the ozone depletion potential for 1-bromopropane using two different methods. First, the semiempirical method of Solomon et al.[16] was used, with a lifetime of 15 days and a nominal bromine efficiency factor of 120. The value of 120 is the product of two factors. Bromine is $\sim$40−50 times more efficient in removing ozone than is chlorine on an atom for atom basis. In addition, the bromopropane molecules release bromine atoms 2−3 times more promptly than CFC-11 would release chlorine atoms in the lower stratosphere as indicated by their respective local lifetimes. Solomon et al. suggest that the ODP should be further discounted by the factor *b*, which is defined as the ratio of the mixing ratio of bromopropane at the tropopause to the mixing ratio at the ground. Our calculation shows that *b* is 0.05, giving an estimated ODP value of 0.0019 in this case.

Our second estimate of bromopropane ODP is obtained using the AER 2-D model which uses the method outlined in ref 17. The results of the calculations depend on the boundary conditions used for bromopropane and Br_y. We obtained an ODP value of 0.027 using a fixed mixing ratio boundary condition for bromopropane with Br_y removed by washout in the lower troposphere and efficient deposition at the ground.

The semiempirical method and the lifetime scaling method were originally derived for species with lifetimes longer than a year. It is highly unlikely that they can be used for species with lifetimes as short as 15 days. Indeed, Prather and Spivakovsky[12] only demonstrated that the method produces credible results if the mixing ratio of the species is constant in the troposphere. The lifetime of a species as short-lived as bromopropane will depend on local OH concentrations rather than the tropospheric average OH concentration; i.e., it will be sensitive to the geographic distribution of emissions. In addition, the ODP calculation is sensitive to tropospheric Br_y removal rates and to transport rates from troposphere to stratosphere.

Acknowledgment. We thank Albemarle Corp. for the support of this work. Partial support was also provided by the NASA Upper Atmospheric Research Program through Contract NAS5-32917.

References and Notes

(1) Abbatt, J. P. D.; Molina, J. M. *Annu. Rev. Energy Environ*. **1993**, *18*, 1−29.

(2) Scientific Assessment of Ozone Depletion: 1991. World Meteorological Organization, Report No. 25, Geneva, Switzerland, 1991.

(3) Scientific Assessment of Ozone Depletion: 1994. World Meteorological Organization, Global Ozone Research and Monitoring Project, Report No. 37, 1995.

(4) Wallington, T. J.; Schneider, W. F.; Worsnop, D. R.; Nielson, O. J.; Sehested, J.; DeBruyn, W. J.; Shorter, J. A. *Environ. Sci. Technol.* **1994**, *28*, 7.

(5) 1995 Methyl Bromide State of the Science Workshop, Workshop Summary, Montery, CA, June 5−7, 1995.

(6) Massie, S. T.; Goldman, A. *J. Quant. Spectrosc. Radiat. Transfer* **1992**, 48, 713−719.

(7) Brown, R. L. *Res. Natl. Bur. Stand*. **1978**, *83*, 1.

(8) *The Aldrich Library of FT-IR Spectra*, 1st ed.; Pouchert, C. J., Ed.; Aldrich Chemical Company: Milwaukee, WI, 1989; Vol. 3.

(9) Donaghy, T.; Shanahan, I.; Hande, M.; Fitzpatrick, S. *Int. J. Chem. Kinet.* **1993**, *25*, 273−284.

(10) Téton, S.; Boudali, A. E.; Mellouki, A. *J. Chem. Phys.* **1996**, *93*, 274−282.

(11) DeMore, W. B.; Sander, S. P.; Golden, D. M.; Hampson, R. F.; Kurylo, M. J.; Howard, C. J.; Ravishankara, A. R.; Kolb, C. E.; Molina, M. J. *Chemical Kinetics and Photochemical Data for Use in Stratospheric Modeling*; JPL Publication 94−26; Jet Propulsion Laboratory, California Institute of Technology: Pasadena, CA, 1994.

(12) Prather, M.; Spivakovsky, C. M. *J. Geophys. Res.* **1990**, *95*, 18723−18729.

(13) Prinn, R.; Weiss, R. F.; Miller, B. R.; Huang, J.; Alyea, F. N.; Cunnold, D. M.; Fraser, P. B.; Hartley, D. E.; Simmonds, P. G. *Science* **1995**, *269*, 187−192.

(14) Butler, J. H.; Elkins, J. W.; Thompson, T. M.; Ball, B. D.; Swanson, T. H.; Koropalov, V. *J. Geophys. Res.* **1991**, *96*, 22347−22355.

(15) Fisher, D. A.; Hales, C. H.; Wang, W.-C.; Ko, M. K. W; Sze, N. D. *Nature* **1990**, *344*, 513−516.

(16) Solomon, S.; Mills, M. J.; Heidt, L. E.; Pollock, W. H.; Tuck, A. F. *J. Geophys. Res.* **1992**, *97*, 825−842.

(17) Fisher, D. A.; Hales, C. H. In *Scientific Assessment of Stratospheric Ozone: 1989. Global Ozone Research and Monitoring Project*; Report No. 20; W*orld Meteorological Organization*: Geneva, 1990; p 385; Vol. II.